

Undersized Mitral Annuloplasty Inhibits Left Ventricular Basal Wall Thickening but Does Not Affect Equatorial Wall Cardiac Strains

Allen Cheng¹, Tom C. Nguyen¹, Marcin Malinowski¹, David Liang², George T. Daughters^{1,3}, Neil B. Ingels, Jr.^{1,3}, D. Craig Miller¹

¹Department of Cardiovascular and Thoracic Surgery, ²Division of Cardiovascular Medicine, Stanford University School of Medicine, Stanford, California, ³Laboratory of Cardiovascular Physiology and Biophysics, Research Institute of the Palo Alto Medical Foundation, Palo Alto, California, USA

Background and aim of the study: Undersized mitral annuloplasty has been widely employed for patients with ischemic mitral regurgitation. Beyond correction of mitral regurgitation, ring annuloplasty is postulated to normalize global left ventricular (LV) shape, thereby decreasing LV wall stress and promoting reverse LV remodeling. The effect of undersized annuloplasty on regional transmural LV wall thickening and strain patterns, however, has not been examined.

Methods: In nine sheep, transmural radiopaque beadsets were inserted into the anterobasal and equatorial lateral LV walls, with additional markers silhouetting the left ventricle and mitral annulus. Four-dimensional marker dynamics were studied with biplane videofluoroscopy (open-chest) before and after tightening a Paneth-type mitral annuloplasty suture. LV volumes, mitral dimensions, transmural circumferential, longitudinal, and radial systolic strains, and end-diastolic (ED) and end-systolic (ES) remodeling strains in the two LV regions were computed.

Undersized mitral ring annuloplasty is widely employed for patients with chronic functional mitral regurgitation (FMR) and ischemic mitral regurgitation (IMR) due to idiopathic or ischemic cardiomyopathy. Besides decreasing mitral regurgitation (MR), annuloplasty is thought to improve global left ventricular (LV) geometry (decrease sphericity), thereby favorably influencing myocardial stresses and strains, which may promote LV reverse remodeling (1,2). Altered

Results: In the anterobasal LV wall close to the mitral annulus, annuloplasty increased ED wall thickness and surprisingly reduced systolic radial strain (wall thickening) at all transmural depths. Radial subepicardial, midwall, and subendocardial wall-thickening strains at ES in the anterobasal LV site were 0.25 ± 0.15 , 0.33 ± 0.16 , and 0.47 ± 0.29 , respectively, before tightening the suture annuloplasty, compared to 0.13 ± 0.12 , 0.15 ± 0.18 , and 0.20 ± 0.26 after tightening. In the equatorial lateral LV wall further away from the annulus, most LV transmural systolic and remodeling strains did not change.

Conclusion: Simulated undersized annuloplasty acutely decreased transmural systolic LV wall thickening in the anterobasal region, without substantially affecting transmural deformations in the lateral LV wall. These acute effects of undersized annuloplasty require a better understanding as they may potentially be deleterious, and a direct ventricular approach may be needed as an adjunct to promote reverse LV remodeling.

The Journal of Heart Valve Disease 2007;16:349-358

myocardial strain patterns, which have been linked with myocyte apoptosis (3-5) and disruption of the extracellular matrix secondary to the activation of matrix metalloproteinases (6-8), may be important factors favoring post-infarction LV remodeling (9-13). The results of recent experiments have shown that an undersized annuloplasty can alter global LV shape by reducing LV circumferential radii of curvature at the basal, equatorial and apical levels, possibly lowering LV wall stress (14), but regional transmural LV wall strain data after mitral annuloplasty are non-existent.

The present study was designed to test the hypothesis that annuloplasty alters regional transmural LV systolic and remodeling strains. To accomplish this goal, transmural beadsets were implanted in two LV regions to examine four-dimensional (4-D) transmural LV biomechanics during reversible acute reduction of mitral annular dimensions in the normal sheep heart.

Presented at the Third Biennial Meeting of the Society for Heart Valve Disease, 17th-20th June 2005, Vancouver Convention and Exhibition Centre, Vancouver, Canada

Address for correspondence:
D. Craig Miller MD, Department of Cardiothoracic Surgery, Falk Cardiovascular Research Center, Stanford University School of Medicine, 300 Pasteur Drive, Stanford, California 94305-5247, USA
e-mail: dcm@stanford.edu

Materials and methods

Animals

Nine sheep adult male Dorsett hybrid sheep (mean body weight 68 ± 5 kg; McGrew Farm, California, USA) were used in these studies. All animals received humane care in compliance with the *Principles of Laboratory Animal Care* formulated by the National Society for Medical Research and the *Guide for Care and Use of Laboratory Animals* prepared by the National Academy of Sciences and published by the National Institutes of Health (DHEW NIHG publication 85-23, revised 1985). This study was approved by the Stanford Medical Center Laboratory Research Animal Review Committee and conducted according to Stanford University policy.

Surgical preparation

The surgical preparation and marker data acquisition methods for these experiments have been described in detail previously (14,15), and therefore will only be briefly mentioned here. Through a left thoracotomy, 13 subepicardial radiopaque markers surgically implanted in each sheep in order to silhouette the LV chamber (Fig. 1). Epicardial echocardiography was used to locate and measure the thickness of the mid-lateral equatorial LV wall between the papillary mus-

cles and another site in the anterobasal LV wall basal to the anterior papillary muscle insertion. Three transmural columns of beads (four beads each, Fig. 1) were then implanted into these two regions using a bead insertion trochar oriented normal to the local epicardial tangent plane. With the animal on cardiopulmonary bypass (CPB), eight radiopaque markers were implanted around the mitral annulus and one marker at each of the mitral leaflet edges. A modified Paneth-Burr annuloplasty suture was then inserted using a double-armed 2-0 polypropylene suture anchored at the left fibrous trigone, suturing around the anterior annulus with pledgets, and exteriorized at the mid-lateral annulus using a tourniquet on the epicardial surface (Fig. 2). A second suture starting at the right fibrous trigone around the posterior annulus was exteriorized on another tourniquet. The animal was weaned from CPB and a micromanometer pressure transducer (PA4.5-X6; Konigsberg Instruments, Inc.) was placed in the ventricle through the apex.

Marker data acquisition

Immediately postoperatively, each animal was taken to the cardiac catheterization laboratory and studied opened-chest, intubated, mechanically ventilated, and anesthetized with isoflurane (1-2.5%). With the heart

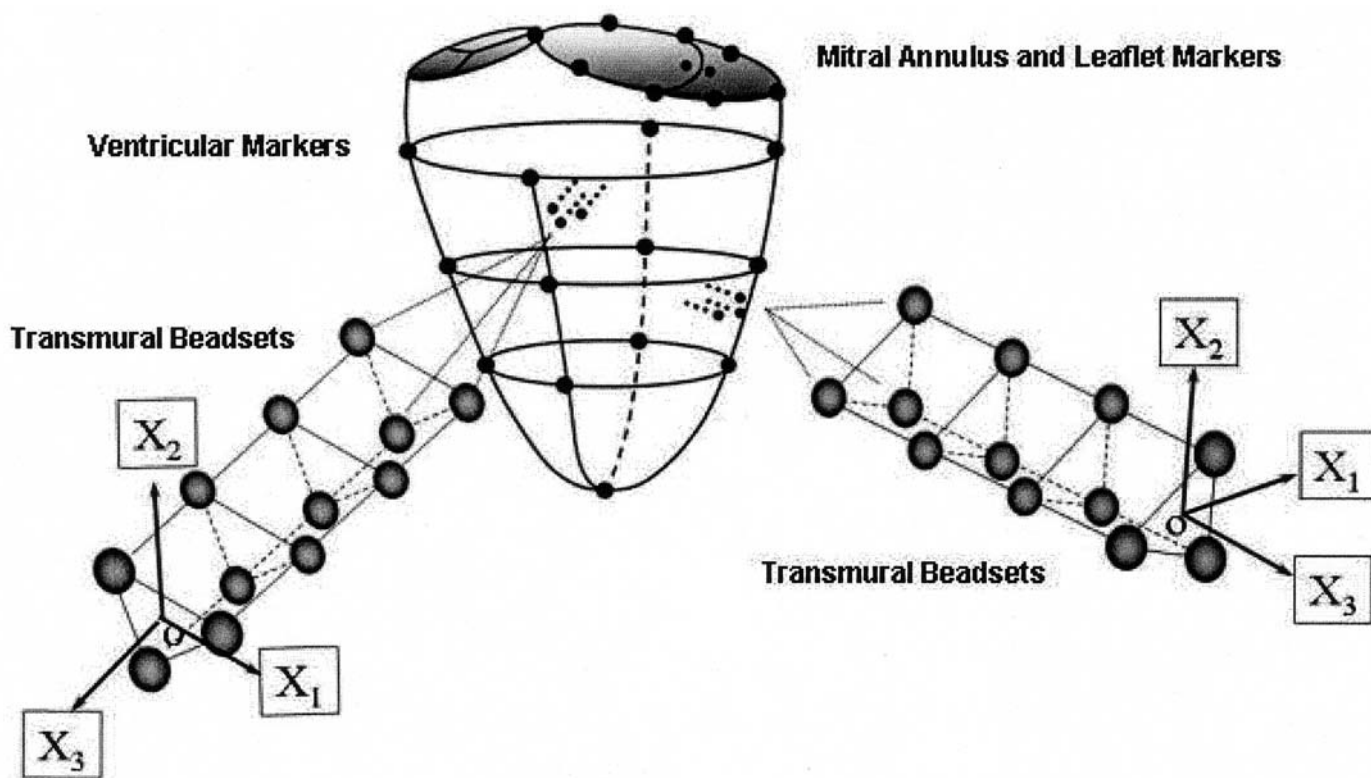


Figure 1: Locations of the LV epicardial markers, LV lateral equatorial and anterior basal transmural beadsets, mitral annulus, and leaflet markers. X_1 , X_2 , and X_3 represent the circumferential, longitudinal, and radial cardiac axis, respectively.

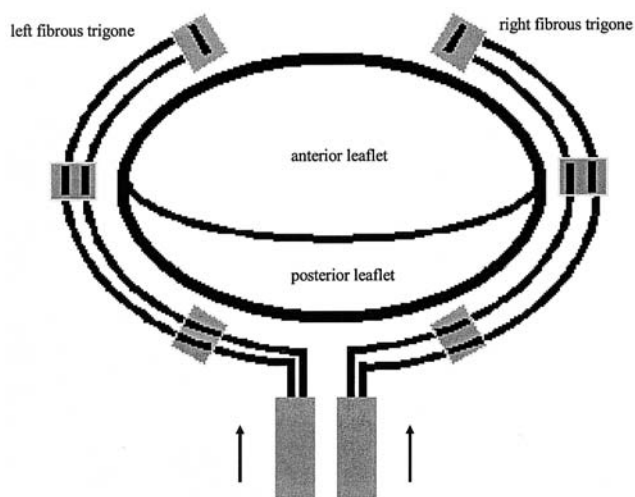


Figure 2: Illustration of the modified Paneth-Burr type suture annuloplasty. The 2-0 double armed polypropylene sutures were anchored at the each fibrous trigone, sutured around the mitral annulus, and exteriorized through the mid-lateral annulus to adjustable tourniquets. (Illustration adapted from Tibayan et al. (14).)

in normal sinus rhythm and ventilation arrested at end-expiration, simultaneous biplane videofluoroscopy (60 Hz), electrocardiogram, and LV and aortic pressures were recorded during steady-state baseline conditions before (Control) and after annular suture pull (ASP) tightening both annular sutures until resistant. Transesophageal echocardiography was used to monitor flow across the mitral valve, and no mitral stenosis or significant changes in gradients across the mitral valve were noted after suture annuloplasty tightening. The decrease in annulus size was confirmed by the change in distance between the annulus radiopaque markers - that is, mid-septal and mid-lateral markers, and anterior and posterior commissures markers. Marker coordinates from the two radiographic views were subsequently digitized and merged to yield three-dimensional (3-D) coordinates for each radiopaque marker every 16.7 ms.

Hemodynamics and cardiac cycle timing

These procedures have been reported previously in detail by Cheng et al. (15). Three consecutive steady-state beats in sinus rhythm were selected for analysis for Control and ASP conditions from each study. The instantaneous left ventricular volume (LVV) was calculated every 16.7 ms from the 3-D coordinates of the epicardial LV markers (Fig. 1) by summing the volumes of multiple space-filling tetrahedra. For each cardiac cycle, end-diastole (ED) was defined as the videofluoroscopic frame immediately prior to the upstroke of the LV pressure curve, defined as LV $dP/dt > 120$ mmHg/s. End-systole (ES) was defined as

the videofluoroscopic frame when LV d^2P/dt^2 changed sign from minus to plus.

Cardiac systolic strains

Strains were reported at 20, 50, and 80% depths from the epicardium, with ED as the reference configuration and ES as the deformed configuration. The detailed strain analysis methodology has been described previously (15). Briefly, a local LV long axis was defined by using the centroid of the three 1.7-mm epicardial surface beads atop the bead columns and the apical marker (Fig. 1), with local cardiac coordinates aligned with the circumferential (X_1), longitudinal (X_2), and radial (X_3) axes of the LV lateral wall. Strains were interpolated along the centroid of the bead columns at 1% increments of wall depth from the epicardium at ED. For each beat, bead positions at ES (deformed configuration) at 20, 50, and 80% wall depth were compared with their positions at ED (reference configuration). In cardiac coordinates (X_1, X_2, X_3), the three normal strain components measured local myocardial stretch or shortening along the circumferential (E_{11}), longitudinal (E_{22}), and radial (E_{33}) cardiac axes. Radial (E_{33}) systolic cardiac strain represented systolic wall thickening. The three shear strains (E_{12}, E_{13} , and E_{23}) represented angle changes between pairs of the originally orthogonal coordinate axes.

End-diastolic and end-systolic cardiac remodeling strains

End-diastolic cardiac remodeling strains were obtained for each heart by comparing bead positions (in cardiac coordinates) at ED from the control study (reference configuration, Control) with the bead posi-

Table I: Mitral annular dimensions during control and annular suture pull (ASP) conditions.

Parameter	Control	ASP
S-L diameter at ES (cm)	2.48 ± 0.21	2.01 ± 0.14*
C-C diameter at ES (cm)	3.60 ± 0.46	2.95 ± 0.42*
S-L _{max} (cm)	2.64 ± 0.34	2.10 ± 0.16
C-C _{max} (cm)	3.88 ± 0.43	3.09 ± 0.42*
S-L _{min} (cm)	2.39 ± 0.19	1.96 ± 0.14*
C-C _{min} (cm)	3.56 ± 0.43	2.90 ± 0.43*

Values are group mean ± SD from nine hearts.

p-values from two-tailed paired *t*-test of control data compared with ASP data; *p < 0.05.

C-C diameter at ES: Commissure-commissure annular diameter at end-systole; C-C_{max}: Maximum commissure-commissure annular diameter; C-C_{min}: Minimum commissure-commissure annular diameter; S-L diameter at ES: Septal-lateral annular diameter at end-systole; S-L_{max}: Maximum septal-lateral annular diameter; S-L_{min}: Minimum septal-lateral annular diameter.

Table II: Transmural anterobasal LV wall systolic cardiac strains at three levels.

Strain/ shear	20% depth		50% depth		80% depth	
	Control	ASP	Control	ASP	Control	ASP
E ₁₁	-0.08 ± 0.08	-0.06 ± 0.06	-0.11 ± 0.09	-0.08 ± 0.06	-0.12 ± 0.08*	-0.07 ± 0.09
E ₂₂	-0.09 ± 0.04	-0.05 ± 0.03	-0.09 ± 0.08	-0.06 ± 0.05	-0.06 ± 0.19	-0.03 ± 0.08
E ₃₃	0.25 ± 0.15 ⁺	0.13 ± 0.12	0.33 ± 0.16 ^{‡§}	0.15 ± 0.18	0.47 ± 0.29 [§]	0.20 ± 0.26
E ₁₂	-0.01 ± 0.03	-0.01 ± 0.02	-0.00 ± 0.04	0.01 ± 0.02	0.02 ± 0.10	0.04 ± 0.06
E ₂₃	0.04 ± 0.09 ⁺	0.03 ± 0.05	0.10 ± 0.09 [‡]	0.07 ± 0.04	0.20 ± 0.21*	0.11 ± 0.06
E ₁₃	-0.02 ± 0.06	0.00 ± 0.04	-0.03 ± 0.08	-0.01 ± 0.04	-0.04 ± 0.16	-0.00 ± 0.09

Values are group mean ± SD from eight hearts.

End-diastole is reference configuration; end-systole is deformed configuration.

^{*}, p < 0.05 Control versus ASP at the same wall depth; [§], p < 0.005 Control versus ASP at the same wall depth; ⁺, p < 0.05 control cardiac strain 20% vs. 80%; [‡], p < 0.07 control cardiac strain 50% versus 80%; from two-way repeated measures ANOVA with Holm-Sidak pairwise multiple comparisons. Depth measured as a percentage of the radial distance from the epicardial bead to the most subendocardial bead.

E₁₁: Circumferential strain; E₂₂: Longitudinal strain; E₃₃: Radial strain; E₁₂: Circumferential-longitudinal shear; E₂₃: Longitudinal-radial shear; E₁₃: Circumferential-radial shear.

tions at ED during suture annuloplasty cinching (deformed configuration, ASP). End-systolic remodeling cardiac strains were obtained for each heart by comparison of bead positions at ES (in cardiac coordinates) from the control study (reference configuration) with the bead positions at ES during tightening of the suture annuloplasty (deformed configuration). In cardiac coordinates (X₁, X₂, X₃), the three normal remodeling strain components measure the change in configuration (Control versus ASP) along the circumferential (E₁₁), longitudinal (E₂₂), and radial (E₃₃) cardiac axes. Radial (E₃₃) remodeling strain represented change of radial wall thickness from Control to ASP configuration. The three shear strains (E₁₂, E₁₃, and E₂₃) represented angle changes between pairs of the originally orthogonal coordinate axes from Control to ASP configuration.

Mitral annular dimensions and dynamics

The commissure-commissure mitral annular diameter was calculated as the distance between the markers at the anterior commissure and posterior commissure in 3-D space (Fig. 1). Septal-lateral annular diameter was calculated as the distance between the septal and mid-lateral annular marker in 3-D space.

Statistical analysis

Cardiac strains were compared using two-way repeated measures ANOVA with Holm-Sidak pairwise multiple comparisons (Sigmastat 3.11, SPSS, Inc., Chicago, IL, USA). Data were reported as mean ± SD. ED and ES strains were compared to zero using a one-sample *t*-test. Group mean annular dimensions and dynamics were compared between baseline and ASP using two-tailed *t*-test for paired observation. A p-value < 0.05 was considered to be statistically significant.

Table III: Changes in transmural LV wall end-diastolic cardiac remodeling strains in the anterobasal region.

Strain/ shear	Control to ASP conditions					
	20% depth		50% depth		80% depth	
		p-value		p-value		p-value
E ₁₁	0.01 ± 0.07	0.58	-0.01 ± 0.08	0.70	-0.04 ± 0.06	0.08
E ₂₂	0.00 ± 0.03	0.81	-0.04 ± 0.04	0.02	-0.06 ± 0.08	0.06
E ₃₃	0.12 ± 0.09	0.006	0.18 ± 0.1	0.001	0.25 ± 0.13	0.001
E ₁₂	0.01 ± 0.03	0.38	0.00 ± 0.03	0.68	0.00 ± 0.03	0.94
E ₂₃	0.01 ± 0.04	0.49	0.01 ± 0.05	0.63	0.02 ± 0.10	0.65
E ₁₃	0.01 ± 0.04	0.47	0.02 ± 0.04	0.19	0.03 ± 0.06	0.18

Values are group mean ± SD from eight hearts.

ED at reference configuration (Control); ED at deformed configuration (ASP).

p-values from two-tailed paired *t*-test compared with zero. Depth measured as a percentage of the radial distance from the epicardial bead to the most subendocardial bead. Strain and shears as defined in Table II.

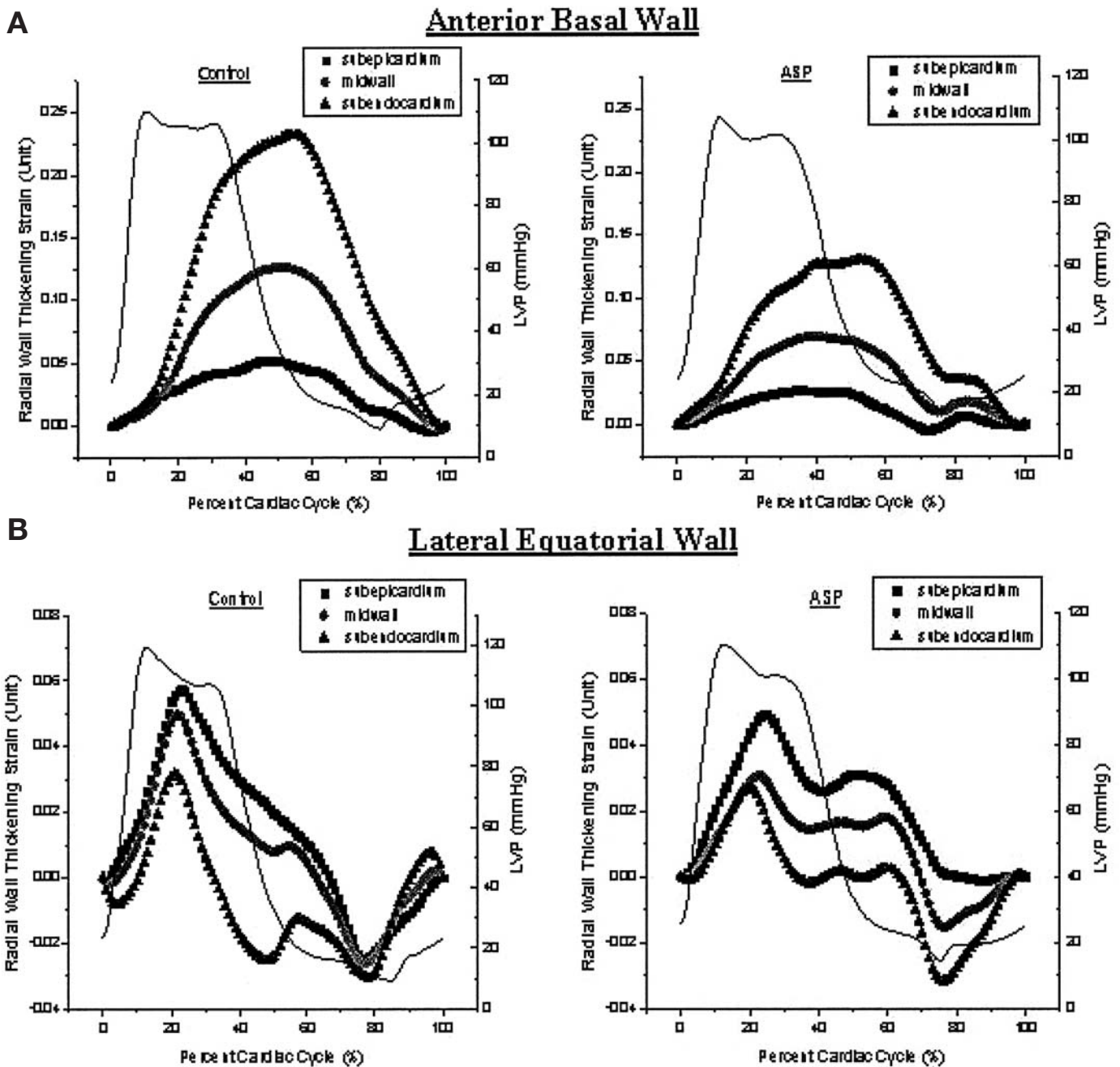


Figure 3: Anterobasal LV radial wall thickening cardiac strain (E_{33}) at 20% (subepicardium), 50% (midwall), and 80% (subendocardium) wall depth from the epicardial surface plotted against time before (Control) and after (ASP) tightening of the adjustable annuloplasty suture. The thin line indicates LV pressure (LVP) plotted versus time.

Results

The changes in mitral annular dimensions between control and ASP conditions are summarized in Table I. ASP decreased both the septal-lateral and the commissure-commissure mitral annular dimensions by approximately 18-20%, as expected.

Systolic cardiac strains in the anterobasal LV wall (ED reference configuration; ES deformed configuration) are summarized in Table II, with data presented

at each of three transmural depths: 20% (subepicardium), 50% (midwall), and 80% (subendocardium). Simulated annuloplasty reduced systolic radial wall thickening (E_{33}) in the anterobasal LV wall closer to the mitral annulus at all transmural depths; ASP also affected the transmural wall thickening gradient (greatest in the subendocardium and least in the subepicardium), longitudinal-radial shear strains at all wall depths, and endocardial circumferential shortening decreased in the anterobasal region.

Table IV: Changes in transmural LV wall end-systolic cardiac remodeling strains in the anterobasal region.

Strain/ shear	Control to ASP conditions					
	20% depth		50% depth		80% depth	
		p-value		p-value		p-value
E ₁₁	0.03 ± 0.04	0.08	0.03 ± 0.03	0.04	0.04 ± 0.07	0.13
E ₂₂	0.04 ± 0.02	0.0002	0.00 ± 0.04	0.92	0.01 ± 0.05	0.61
E ₃₃	0.03 ± 0.04	0.10	0.04 ± 0.05	0.048	0.05 ± 0.046	0.01
E ₁₂	0.01 ± 0.02	0.13	0.01 ± 0.03	0.33	-0.01 ± 0.03	0.18
E ₂₃	-0.01 ± 0.03	0.45	-0.01 ± 0.03	0.27	-0.01 ± 0.03	0.25
E ₁₃	0.02 ± 0.03	0.04	0.03 ± 0.03	0.02	0.03 ± 0.05	0.10

Values are group mean ± SD from eight hearts.

ED at reference configuration (Control); ES at deformed configuration (ASP).

p-values from two-tailed paired *t*-test compared with zero. Depth measured as a percentage of the radial distance from the epicardial bead to the most subendocardial bead. Strain and shears as defined in Table II.

The cardiac ED and ES remodeling strains in the anterobasal LV region are summarized in Tables III and IV, respectively. Wall thickness (E₃₃ remodeling strain) at ED was significantly increased with ASP at all transmural depths, and wall thickening increased only slightly at ES (4% in the midwall, 5% in the subendocardium). Taken together, these changes explain the fall in systolic wall thickening near the annulus in the anterobasal LV wall.

The group mean radial wall thickening strains (E₃₃) throughout the cardiac cycle at the three wall depths in the anterobasal and lateral equatorial LV regions are illustrated in Figure 3. Systolic transmural radial wall thickening fell during annuloplasty (ASP). It should be noted that the Control values of E₃₃ were much larger in the anterobasal region compared to the lateral wall, such that ASP reduced anterobasal E₃₃ to the lower range observed in the lateral equatorial region during both Control and ASP conditions.

The systolic cardiac strains in the equatorial lateral

LV wall are summarized in Table V. Being further away from the annulus, no significant changes in systolic cardiac normal strain or shear strain occurred in this region after tightening suture annuloplasty. In this equatorial lateral region, annuloplasty tightening increased transmural longitudinal ED remodeling strain (3%) and subendocardial ES remodeling strain (6%), which indicated that ASP lengthened the lateral equatorial wall slightly at ED and ES. However, ASP did not affect the other cardiac normal or shear remodeling strains either at ED or ES (Tables VI and VII).

Discussion

Undersized mitral ring annuloplasty is offered to selected patients with dilated or ischemic cardiomyopathy who also have chronic FMR or IMR. Undersized annuloplasty has been shown to optimize LV geometry and decrease LV sphericity, and hence may potentially reduce LV wall stress (1,2,16). Tibayan

Table V: Transmural LV wall systolic cardiac strains in the equatorial lateral region.

Strain/ shear	20% depth		50% depth		80% depth	
	Control	ASP	Control	ASP	Control	ASP
E ₁₁	-0.06 ± 0.05*	-0.04 ± 0.05*	-0.09 ± 0.06+	-0.08 ± 0.05+	-0.16 ± 0.08	-0.15 ± 0.07
E ₂₂	-0.01 ± 0.03	-0.01 ± 0.03	-0.05 ± 0.04	-0.05 ± 0.04	-0.11 ± 0.03	-0.10 ± 0.05
E ₃₃	0.13 ± 0.03*	0.11 ± 0.05*	0.20 ± 0.11+	0.18 ± 0.09+	0.30 ± 0.24	0.27 ± 0.19
E ₁₂	0.04 ± 0.03	0.04 ± 0.03	0.06 ± 0.03	0.06 ± 0.04	0.07 ± 0.05	0.07 ± 0.05
E ₂₃	0.04 ± 0.06	0.03 ± 0.05	0.02 ± 0.04	0.02 ± 0.04	-0.01 ± 0.10	-0.00 ± 0.08
E ₁₃	0.03 ± 0.05	0.02 ± 0.05	0.06 ± 0.05	0.04 ± 0.05	0.10 ± 0.06	0.07 ± 0.05

Values are group mean ± SD from eight hearts.

End-diastole is reference configuration; end-systole is deformed configuration.

*p < 0.05 cardiac strain 20% vs. 80%; +p < 0.05 control cardiac strain 50% vs. 80%.

From two-way repeated measures ANOVA with Holm-Sidak pairwise multiple comparisons. Depth measured as a percentage of the radial distance from the epicardial bead to the most subendocardial bead. Strain and shears as defined in Table II.

Table VI: Changes in transmural LV wall end-diastolic cardiac remodeling strains in the equatorial lateral region.

Strain/ shear	Control to ASP					
	20% depth	p-value	50% depth	p-value	80% depth	p-value
E ₁₁	0.00 ± 0.02	0.95	-0.00 ± 0.02	0.63	-0.00 ± 0.04	0.95
E ₂₂	0.03 ± 0.02	0.0046	0.03 ± 0.02	0.023	0.03 ± 0.03	0.024
E ₃₃	0.05 ± 0.07	0.11	0.05 ± 0.09	0.21	0.05 ± 0.14	0.37
E ₁₂	0.01 ± 0.01	0.23	-0.00 ± 0.01	0.86	-0.01 ± 0.03	0.22
E ₂₃	0.01 ± 0.03	0.63	0.01 ± 0.03	0.52	0.00 ± 0.03	0.81
E ₁₃	-0.01 ± 0.02	0.12	-0.00 ± 0.01	0.4	-0.00 ± 0.01	0.48

Values are group mean ± SD from eight hearts.

ED at reference configuration (Control); ED at deformed configuration (ASP).

p-values from two-tailed paired *t*-test compared with zero. Depth measured as a percentage of the radial distance from the epicardial bead to the most subendocardial bead. Strain and shears as defined in Table II.

et al. (14), from the present authors' laboratory, showed that simulated mitral annuloplasty decreased LV circumferential radii of curvature at the basal, equatorial, and apical levels which, according to the law of La Place, should reduce LV wall stress. Precise regional transmural LV wall strains, however, have not been measured before and after undersized mitral annuloplasty.

The ability to alter myocardial strains favorably is important for any surgical approach aimed at promoting reverse LV remodeling. Altered wall strain is associated with the production of inflammatory cytokines and reactive oxygen species, which in turn stimulate myocyte apoptosis, matrix metalloproteinases activation causing extracellular matrix disruption, and fibrosis, which are triggers catalyzing further global LV dilatation, shape change and remodeling. Altered wall strain has also been proposed to be linked with infarct extension, which can initiate LV remodeling (9,10). Regional LV dysfunction, which initially is localized to the infarct, extends to the remainder of the ventricle

and converts normally perfused myocardium into dysfunctional myocardium. Jackson et al. (10) showed that shear strain alterations occur both in myocardium adjacent to and remote from the infarct myocardium in a chronic model. Progressive LV dilatation and LV chamber sphericalization can lead to increased myocyte stretching; subsequently, the heart may enter into an adverse positive feedback loop of dilatation and further exaggerated wall stress.

Despite the current popularity of undersized mitral annuloplasty, recent clinical studies in patients with IMR have shown that MR frequently recurs secondary to ongoing and progressive LV remodeling (17-20), with suboptimal mid-term survival (21-23). Recurrent MR is often due to continued LV remodeling and global dilatation, further papillary muscle displacement, and more leaflet apical tethering. The effects of undersized annuloplasty on LV wall strain are germane to assess whether this can reverse LV wall remodeling sufficiently by preventing strain alteration in infarct extension and/or activation of injurious neurohu-

Table VII: Changes in transmural LV wall end-systolic cardiac remodeling strains in the equatorial lateral region.

Strain/ shear	Control to ASP					
	20% depth	p-value	50% depth	p-value	80% depth	p-value
E ₁₁	0.02 ± 0.03	0.20	0.02 ± 0.02	0.13	0.02 ± 0.04	0.17
E ₂₂	0.02 ± 0.04	0.21	0.02 ± 0.05	0.29	0.06 ± 0.06	0.048
E ₃₃	0.03 ± 0.05	0.12	0.03 ± 0.07	0.26	0.03 ± 0.10	0.48
E ₁₂	-0.00 ± 0.03	0.87	-0.00 ± 0.03	0.88	-0.02 ± 0.03	0.11
E ₂₃	-0.00 ± 0.03	0.89	-0.01 ± 0.02	0.24	-0.02 ± 0.05	0.22
E ₁₃	-0.02 ± 0.02	0.045	-0.01 ± 0.02	0.42	0.02 ± 0.04	0.28

Values are group mean ± SD from eight hearts.

ES at reference configuration (Control); ES at deformed configuration (ASP).

p-values from two-tailed paired *t*-test compared with zero. Depth measured as a percentage of the radial distance from the epicardial bead to the most subendocardial bead. Strain and shears as defined in Table II.

moral cascades.

After simulation of an undersized annuloplasty, the LV wall at ED in the anterobasal region was thicker (E_{33} remodeling strain) and had less systolic wall thickening (E_{33} systolic strain). This implies indirectly that the overcorrection of mitral annular dimensions has an adverse effect on LV systolic function in the basal LV region near the annulus. Previous studies have shown that annuloplasty rings abolish normal mitral annular dynamics (24) and restrict the posterior mitral leaflet closing motion (25). It will be of concern if undersized annuloplasty is confirmed to have an adverse effect on basal LV wall thickening mechanics in human subjects. The inhibition of basal systolic function may further contribute to the continued LV remodeling and global dilatation in patients after surgical repair of IMR. Both the mitral septal-lateral and commissure-commissure dimensions were reduced by 20% in this experiment. The newer annuloplasty rings, with more aggressive downsizing, such as the Edwards IMR ETlogix and Geoform rings and St. Jude Medical Rigid Saddle ring (RSR) which disproportionally downsized the mitral septal-lateral annular dimension, on basal LV wall thickening are unknown and will require further study.

In the present study, the effects of undersized annuloplasty on transmural LV strain patterns in two different regions were explored in order to evaluate its potential effects in terms of reverse LV remodeling. Undersized annuloplasty decreased endocardial longitudinal-radial shear strain in the anterobasal region; however, further away from the mitral annulus, it did not affect systolic strains and increased longitudinal ED and ES remodeling normal strain only slightly in the equatorial lateral LV wall. Hence, in this simulated acute model of undersized annuloplasty in the normal sheep heart, annular reduction has different effects on myocardial strains in these two LV regions. Ischemic mitral regurgitation is a manifestation of myocardial infarction and subsequent infarction-induced LV remodeling. However, the correction of MR by undersized annuloplasty, as suggested in the present experiment, may not be sufficient to correct strain perturbation in myocardium away from the mitral annulus. Previous studies have suggested that MR may only be a manifestation of ventricular remodeling in IMR (26). A direct ventricular approach to reduce wall stress will probably be necessary as an adjunct to promote reverse remodeling. The results of other studies (11,12) have shown that alteration in cardiac strains occurred and persisted after myocardial infarction in LV remodeling. Alterations in shear strain (longitudinal-radial and circumferential-radial) were noted in both the regions adjacent to and remote from the infarcted myocardium (11). Based on the results of the

present study, and because undersized annuloplasty did not alter systolic cardiac strains and remodeling strains further from the annulus at the equatorial level, it is conjectured that undersized annuloplasty alone would not be sufficient to correct the increased shear strains as seen in the chronic model. A combined ventricular surgical approach plus ring annuloplasty might therefore be necessary to repair annular dilatation, leaflet tethering, and altered shear strains, as observed in chronic IMR or FMR. Further investigation of these issues is needed. Multiple surgical ventricular approaches aimed at promoting reverse LV remodeling have been proposed (26-29), and treatments that directly change LV shape and wall stress appear to be potentially important. For example, a randomized clinical trial has recently shown encouraging results using passive ventricular constraint (Acorn CorCap cardiac support device (CSD); Acorn Cardiovascular, St. Paul, MN, USA) as an adjunct to mitral valve repair or replacement in patients with congestive heart failure (CHF) and FMR due to non-ischemic etiologies (30) by demonstrating that a CSD plus ring annuloplasty resulted in progressively smaller LV ES and ED volumes and a more elliptical LV shape over time. Combined surgical treatment also reduced the need for major cardiac procedures and improved the patients' quality of life. Experimental studies have also demonstrated a beneficial effect of CSD in reducing CHF progression in animal models of CHF (31-34).

The possible deleterious effect of annuloplasty in terms of LV anterobasal wall systolic thickening along with no discernable reverse remodeling in the LV equatorial wall in this acute experiment should be considered in the design of newer surgical interventions. A direct ventricular procedure to minimize transmural LV strain perturbations remote from the LV base is probably needed as an adjunct to undersized annuloplasty to promote reverse LV remodeling.

Study limitations

Several limitations are inherent in this experiment, and the results of this acute open-chest experiment in normal sheep hearts cannot be applied strictly to the clinical scenario of chronic IMR or FMR in human patients with CHF.

Ischemia or infarction was not induced in this study in order to allow examination of the isolated effects of simulated annuloplasty on myocardial strains. A recent study from the present authors' laboratory has shown that myocardial infarction causes shear strain alterations in both regions adjacent to and remote from the infarct (11). It should be noted, however, that the systolic and remodeling cardiac strain data in this acute study was very similar to those in a previously reported chronic model (11).

In the present experiment, the effect of reversible simulated undersized mitral annuloplasty was only examined in order to allow direct comparison of baseline and annuloplasty data in the same hearts. Future investigations are needed to examine different annuloplasty (especially rigid) rings, which may alter systolic basal wall thickening to an even greater degree. It should be noted that the septal-lateral and commissure-commissure dimensions with ASP in the present study were reduced by approximately 18-20%, but additional experiments are needed to examine annuloplasty rings with more aggressive septal-lateral downsizing. Disproportional ring downsizing (e.g., septal-lateral, which is intrinsic in the design of the IMR ETlogix, Geoform, and RSR rings) may avoid the deleterious effect on basal systolic wall thickening and LV remodeling.

Only two myocardial regions were assessed in this study. Placement of more than two transmural beadsets is difficult to visualize with biplane videofluoroscopy throughout the cardiac cycle. Ultimately, magnetic resonance imaging (MRI) should prove to be the best method for this type of experiment, as it allows assessment of the entire ventricle rather than selected regions; however, the current spatial resolution of MRI is inadequate to make the required measurements for direct comparison to the presently observed data. Most reports with MRI have reported average strain contributions over the entire transmural thickness at each LV site, or have used model assumptions for each LV wall depth. If the transmural thickness of the LV wall is 10 mm, and the aim is to resolve the strains of one third of the wall (3 mm) within 0.05 mm, this would require a spatial resolution of 0.15 mm (0.05 ± 3 mm), which is available in the present bead column studies, but not with MRI.

Acknowledgements

The authors appreciate the superb technical assistance provided by Mary K. Zasio, Maggie Brophy, and Mark Grisedale. They also thank Drs. James W. Covell, Andrew D. McCulloch, and Jeffrey H. Omens at the University of California, San Diego.

These studies were supported by Grants HL-29589 and HL-67025 from the National Heart, Lung and Blood Institute. Dr. Cheng and Nguyen were Carl and Leah McConnell Cardiovascular Surgical Research Fellows. Dr. Cheng was a recipient of the Thoracic Society Foundation Research Fellowship Award.

References

1. Bach DS, Bolling SF. Improvement following correction of secondary mitral regurgitation in end-stage cardiomyopathy with mitral annuloplasty. *Am J Cardiol* 1196;78:966-969
2. Bolling SF, Pagani FD, Deeb GM, Bach DS. Intermediate-term outcome of mitral reconstruction in cardiomyopathy. *J Thorac Cardiovasc Surg* 1998;115:381-386
3. Kang PM, Izumo S. Apoptosis and heart failure - A critical review of the literature. *Circ Res* 2000;86:1107-1113
4. Saraste A, Pulkki K, Kallajoki M, Henriksen K, Parvinen M, Voipio Pulkki LM. Apoptosis in human acute myocardial infarction. *Circulation* 1997;95:320-323
5. Olivetti G, Abbi R, Quaini F, et al. Apoptosis in the failing human heart. *N Engl J Med* 1997;336:1131-1141
6. Tyagi SC, Lewis K, Pikes D, et al. Stretch-induced membrane type matrix metalloproteinase and tissue plasminogen activator in cardiac fibroblast cells. *J Cell Physiol* 1998;176:374-382
7. Wilson EM, Moainie SL, Baskin JM, et al. Region and species specific induction of matrix metalloproteinases occurs with post myocardial infarction remodeling. *Circulation* 2002;106:345
8. Bowen FW, Jones SC, Narula N, et al. Restraining acute infarct expansion decreases collagenase activity in borderzone myocardium. *Ann Thorac Surg* 2001;72:1950-1956
9. Ratcliffe MB. Non-ischemic infarct extension: A new type of infarct enlargement and a potential therapeutic target. *J Am Coll Cardiol* 2002;40:1168-1171
10. Jackson BM, Gorman JH, Moainie SL, et al. Extension of borderzone myocardium in postinfarction dilated cardiomyopathy. *J Am Coll Cardiol* 2002;40:1160-1167
11. Cheng A, Langer F, Malinowski M, et al. Transmural shear strains alteration adjacent to and remote from infarcted myocardium. *J Heart Valve Dis* 2006;15:209-218
12. Rodriguez F, Langer F, Harrington KB, et al. Alterations in transmural strains adjacent to ischemic myocardium during acute midcircumflex occlusion. *J Thorac Cardiovasc Surg* 2005;129:791-803
13. Moulton MJ, Downing SW, Creswell LL, et al. Mechanical dysfunction in the border zone of an ovine model of left-ventricular aneurysm. *Ann Thorac Surg* 1995;60:986-998
14. Tibayan FA, Rodriguez F, Langer F, et al. Undersized mitral annuloplasty alters left ventricular shape during acute ischemic mitral regurgitation. *Circulation* 2004;110:II98-II102
15. Cheng A, Langer F, Rodriguez F, et al. Transmural cardiac strains in the lateral wall of the ovine left ventricle. *Am J Physiol Heart Circ Physiol* 2005;288:H1546-H1556

16. Romano M, Bolling SF. Update on mitral repair in dilated cardiomyopathy. *J Cardiac Surg* 2004;19:396-400
17. Matsunaga A, Tahta SA, Duran CMG. Failure of reduction annuloplasty for functional ischemic mitral regurgitation. *J Heart Valve Dis* 2004;13:390-397
18. Mcgee EC, Gillinov AM, Blackstone EH, et al. Recurrent mitral regurgitation after annuloplasty for functional ischemic mitral regurgitation. *J Thorac Cardiovasc Surg* 2004;128:916-924
19. Diodato MD, Moon MR, Pasque MK, et al. Repair of ischemic mitral regurgitation does not increase mortality or improve long-term survival in patients undergoing coronary artery revascularization: A propensity analysis. *Ann Thorac Surg* 2004;78:794-799
20. Tolis GA, Korkolis DP, Kopf GS, Elefteriades JA. Revascularization alone (without mitral valve repair) suffices in patients with advanced ischemic cardiomyopathy and mild-to-moderate mitral regurgitation. *Ann Thorac Surg* 2002;74:1476-1481
21. Wu AH, Aaronson KD, Bolling SF, Pagani FD, Welch K, Koelling TM. Impact of mitral valve annuloplasty on mortality risk in patients with mitral regurgitation and left ventricular systolic dysfunction. *J Am Coll Cardiol* 2005;45:381-387
22. Harris KM, Sundt TM, Aeppli D, Sharma R, Barzilai B. Can late survival of patients with moderate ischemic mitral regurgitation be impacted by intervention on the valve? *Ann Thorac Surg* 2002;74:1468-1475
23. Filsoufi F, Aklog L, Byrne JG, Cohn LH, Adams DH. Current results of combined coronary artery bypass grafting and mitral annuloplasty in patients with moderate ischemic mitral regurgitation. *J Heart Valve Dis* 2004;13:747-753
24. Glasson JR, Green GR, Nistal JF, et al. Mitral annular size and shape in sheep with annuloplasty rings. *J Thorac Cardiovasc Surg* 1999;117:302-309
25. Green GR, Dagum P, Glasson JR, et al. Restricted posterior leaflet motion after mitral ring annuloplasty. *Ann Thorac Surg* 1999;68:2100-2106
26. Enomoto Y, Gorman JH, Moainie SL, et al. Surgical treatment of ischemic mitral regurgitation might not influence ventricular remodeling. *J Thorac Cardiovasc Surg* 2005;129:504-511
27. Oz MC, Konertz WF, Kleber FX, et al. Global surgical experience with the acorn cardiac support device. *J Thorac Cardiovasc Surg* 2003;126:983-991
28. Fukamachi K, Inoue M, Popovic Z, et al. Optimal mitral annular and subvalvular shape change created by the coapsys device to treat functional mitral regurgitation. *Am Soc Artif Intern Organs J* 2005;51:17-21
29. Kaza AK, Patel MR, Fiser SM, et al. Ventricular reconstruction results in improved left ventricular function and amelioration of mitral insufficiency. *Ann Surg* 2002;235:828-831
30. Acker MA, Bolling SF, Mann DL, et al. Mitral valve surgery in heart failure: Insights from the Acorn CorCap trial. *J Thorac Cardiovasc Surg* 2006;132:568-577
31. Chaudhry PA, Anagnostopoulos PV, Mishima T, et al. Acute ventricular reduction with the Acorn cardiac support device: Effect on progressive left ventricular dysfunction and dilation in dogs with chronic heart failure. *J Cardiac Surg* 2001;16:118-126
32. Chaudhry PA, Mishima T, Sharov VG, et al. Passive epicardial containment prevents ventricular remodeling in heart failure. *Ann Thorac Surg* 2000;70:1275-1280
33. Saavedra WF, Tunin RS, Paolocci N, et al. Reverse remodeling and enhanced adrenergic reserve from passive external support in experimental dilated heart failure. *J Am Coll Cardiol* 2002;39:2069-2076
34. Power JM, Raman J, Dornom A, et al. Passive ventricular constraint amends the course of heart failure: A study in an ovine model of dilated cardiomyopathy. *Cardiovasc Res* 1999;44:549-555

Meeting discussion

DR. AJIT YOGANATHAN (Atlanta, Georgia, USA): How long after their placement were the rings imaged? Was this done immediately?

DR. ALLEN CHENG (Stanford, California, USA): The sutured annuloplasty was performed in the operating room, and the sheep were then transferred to the catheter laboratory. Biplane video fluoroscopy images were then taken to record the dynamics of the myocardium before the sutured annuloplasty was cinched down. We then performed another run, after the annuloplasty was cinched down again, and the two were compared.

DR. YOGANATHAN: But was that was done immediately?

DR. CHENG: There was about a 10-minute gap in between recordings.